iNOS aggravates pressure overload-induced cardiac dysfunction via activation of the cytosolic-mtDNA-mediated cGAS-STING pathway

Running title: cytosolic mtDNA and cGAS-STING pathway in cardiac dysfunction

Yongzheng Guo[1], Yuehua You[1], Fei-Fei Shang[2], Xiaowen Wang[3], Bi Huang[1], Boying Zhao[4], Dingyi Lv[1], Shenglan Yang[1], Ming Xie[4], Lingwen Kong[4], Dingyuan Du[4], Suxin Luo[1*], Xin Tian[5*] and Yong Xia[1,2,6*]

[1]Division of Cardiology, The First Affiliated Hospital of Chongqing Medical University, Chongqing 400016, China;
[2]Institute of Life Science, Chongqing Medical University, Chongqing 400016, China;
[3]Department of Cardiothoracic Surgery, The First Affiliated Hospital of Chongqing Medical University, Chongqing 400016, China;
[4] Department of Cardiothoracic Surgery, Chongqing University Central Hospital, Chongqing 400014, China;
[5]Department of Neurology, The First Affiliated Hospital of Chongqing Medical University, Chongqing Key Laboratory of Neurology, Chongqing 400016, China;
[6]Davis Heart & Lung Research Institute, Division of Cardiovascular Medicine, The Ohio State University College of Medicine, OH 43210, USA.

***Address for Correspondence:** E-mail: yong.xia@osumc.edu (Yong Xia) ; xintian@cqmu.edu.cn (Xin Tian); luosuxin@hospital.cqmu.edu.cn

This file includes:

Supplemental Fig.1-10

Supplemental Table 1

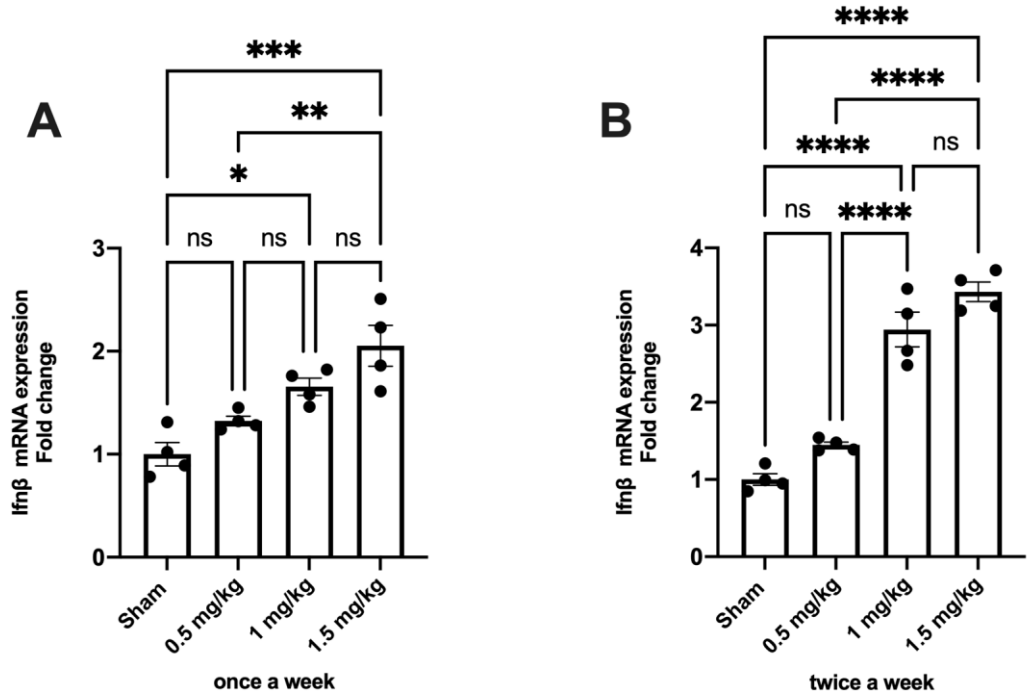

Figure S1. (A-B) mice we subjected to STING agonist at different dosage for once a week or twice a week for 4 weeks. The the IFNβ mRNA expression in heart was measured. The results showed that the dosage of 1 mg/kg STING agonist by intravenous injection twice a week increased the IFNβ expression in heart more effectively, n = 4. Values are means ± SEM. Data were analyzed using a one-way ANOVA with a Tukey's multiple-comparison post-hoc test. *, $P < 0.05$. **, $P < 0.01$. ***, $P < 0.001$. ****, $P < 0.0001$.

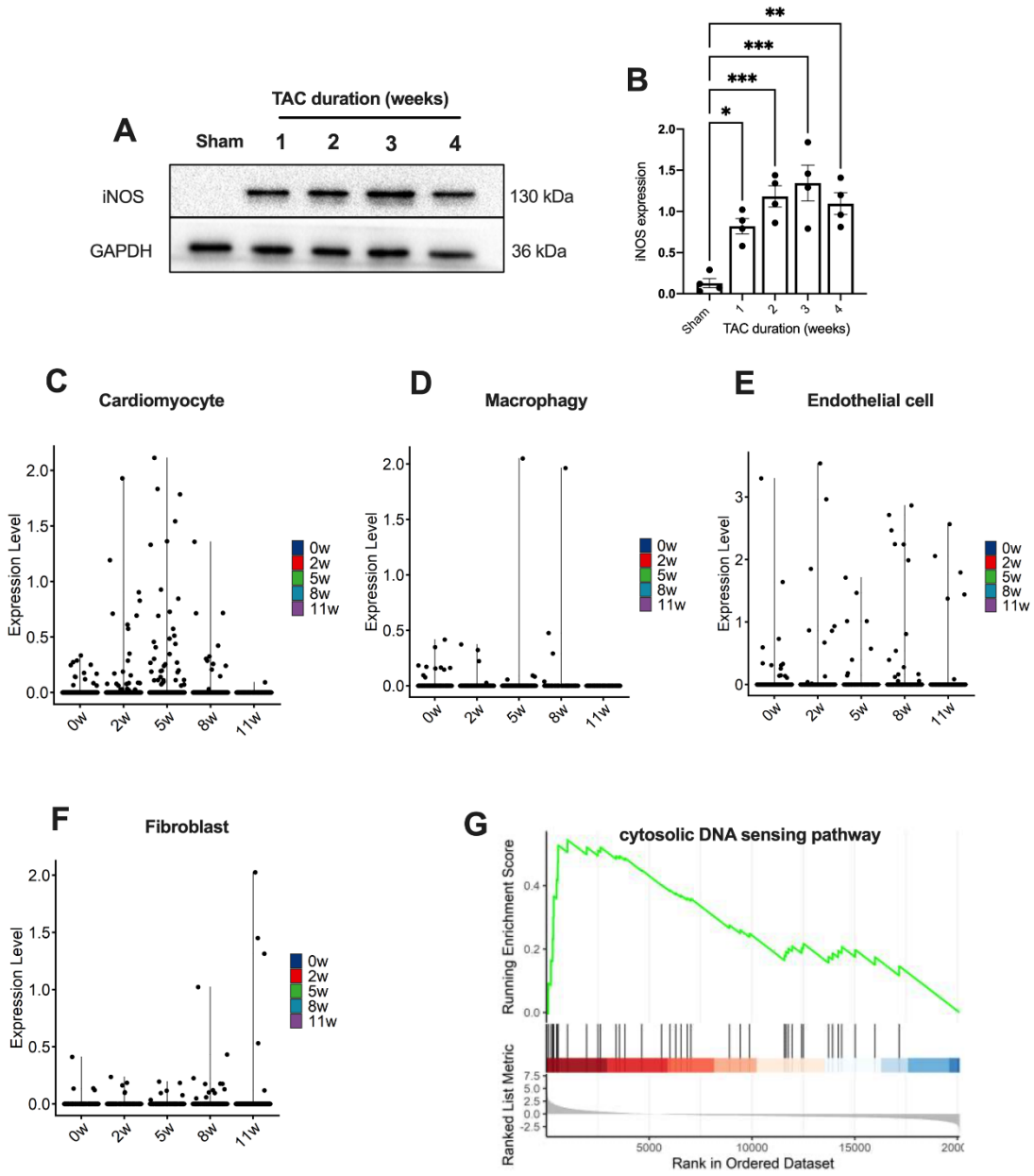

Figure S2. (A-B) Pressure overload increased iNOS expression in the heart, n = 4. **(C-F)** The single-cell sequencing results showed that iNOS expression mainly increased in cardiomyocytes **(C)**, but not in macrophages **(D)**, endothelial cell **(E)** and fibroblast **(F)**. **(G)** Gene set enrichment analysis indicated that the differentially expressed genes were primarily associated with cytosolic DNA pathway in TAC heart. Values are means ± SEM. Data were analyzed using a one-way ANOVA with a Tukey's multiple-comparison post-hoc test. *, $P < 0.05$. **, $P < 0.01$. ***, $P < 0.001$.

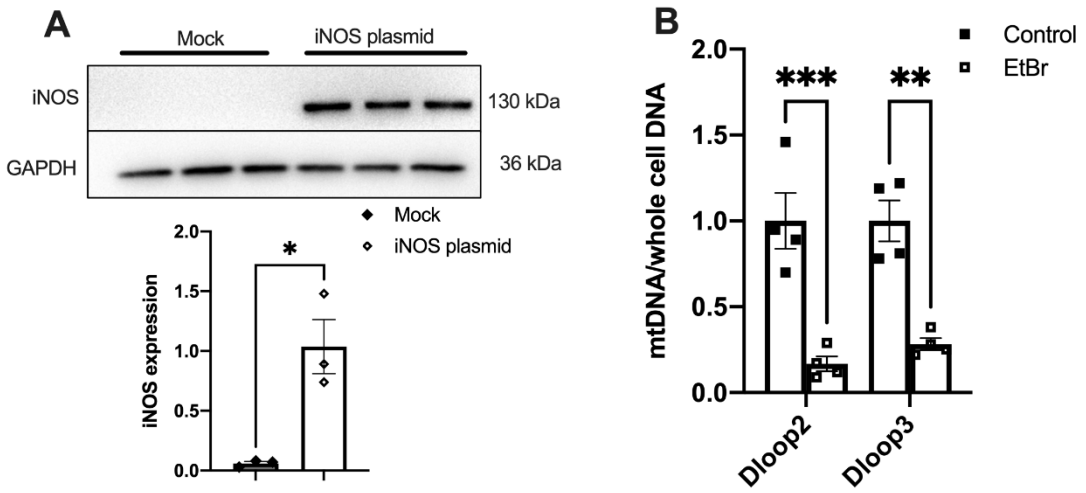

Figure S3. (A) Plasmid encoding iNOS was transfected into isolated cardiomyocytes to overexpress iNOS, and the western blots showed an increased iNOS expression in cardiomyocytes, n = 3; **(B)** EtBr was used to deplete mtDNA in H9C2 cells, n = 4. Values are means ± SEM. Data were analyzed using a one-way ANOVA with a Tukey's multiple-comparison post-hoc test. *, $P < 0.05$. **, $P < 0.01$. ***, $P < 0.001$.

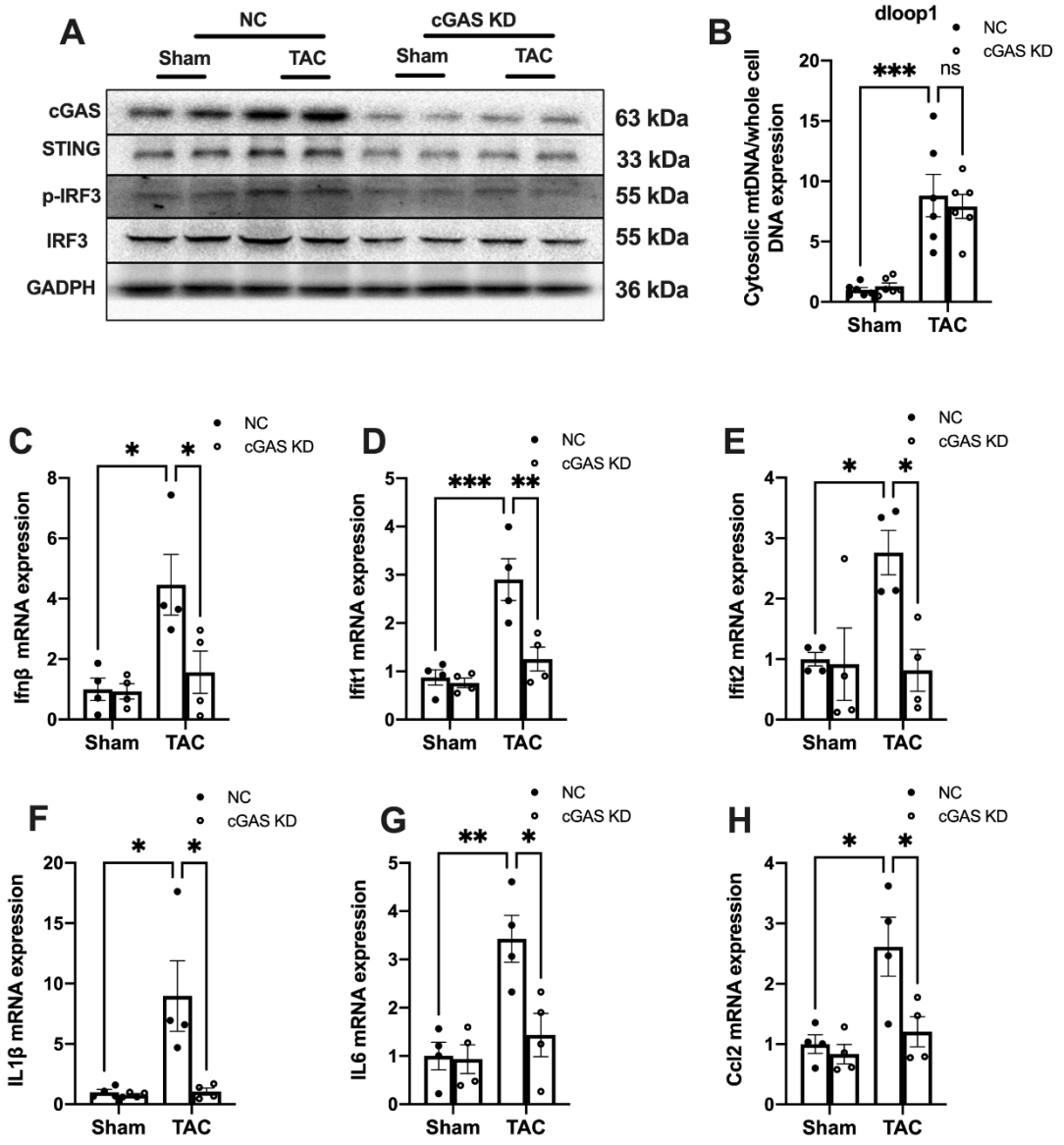

Figure S4. (A) Knockdown of cGAS suppresses the phosphorylation of IRF3 in TAC hearts, n = 6. **(B)** Cytosolic mtDNA content in the heart of TAC mice were measured using quantitative-PCR, n = 6. **(D-E)** Quantitative-PCR was performed to measure the transcript levels of IFN-β and ISGs activated by cGAS-STING, n = 4. **(F-H)** cGAS knockdown suppresses the expression of inflammatory markers in TAC heart, n = 4. Data are presented as the mean ± SEM. Data were analyzed using a two-way ANOVA with a Tukey's multiple-comparison post-hoc test. *, $P < 0.05$. ***, $P < 0.001$. ****, $P < 0.0001$.

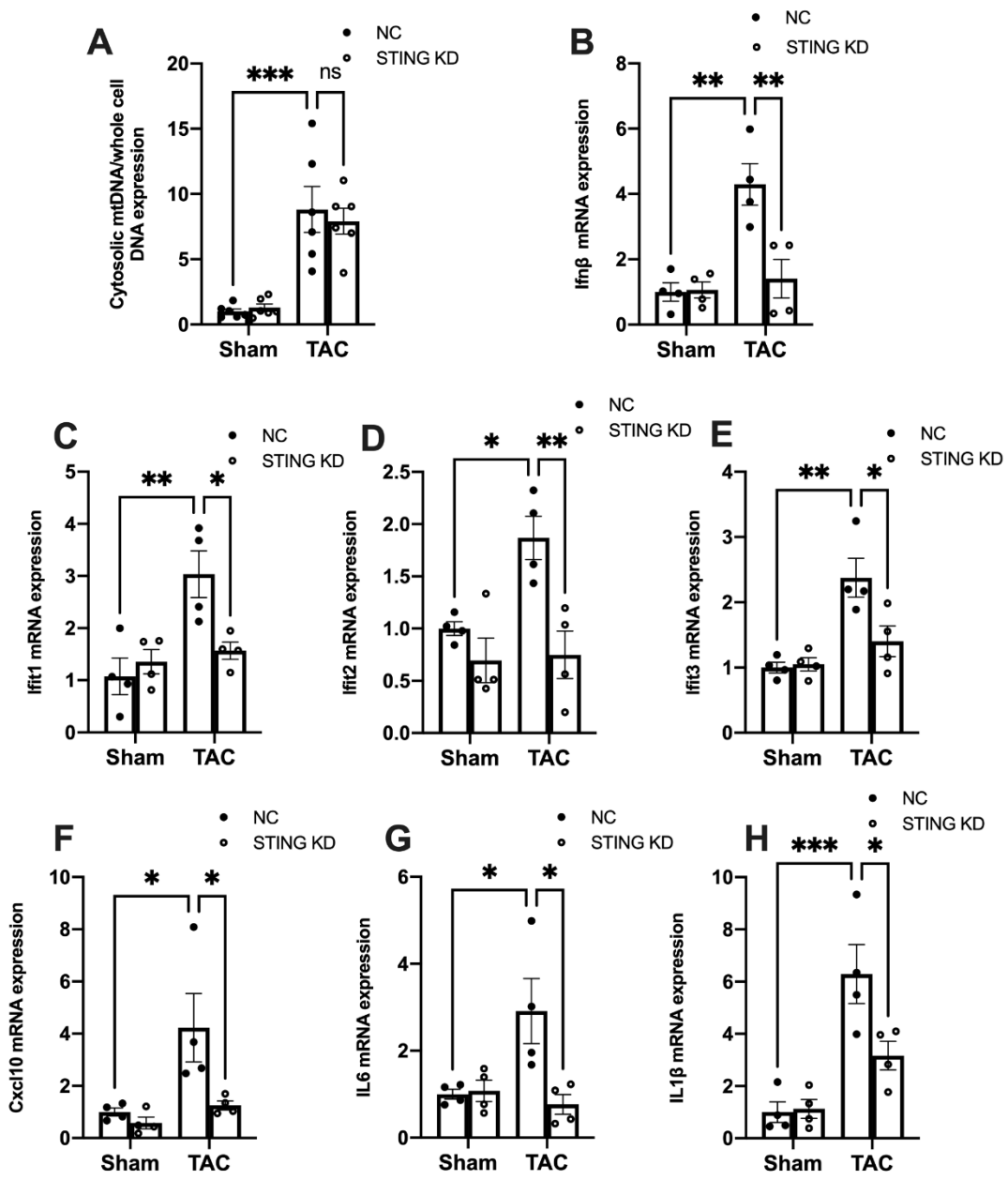

Figure S5. (A) Cytosolic mtDNA content in the heart of TAC mice were measured using quantitative-PCR, n = 6. **(B)** Quantitative-PCR was used to measure the transcript levels of IFN-β activated by cGAS-STING, n = 4. **(D-E)** STING knockdown suppressed the transcript levels of ISGs activated by cGAS-STING in TAC heart, n = 4. **(F-H)** STING knockdown suppressed the expression of inflammatory markers in TAC heart, n=4. Data are presented as the mean ± SEM. Data were analyzed using a two-way ANOVA with a Tukey's multiple-comparison post-hoc test. *, $P < 0.05$. **, $P < 0.01$. ***, $P < 0.001$.

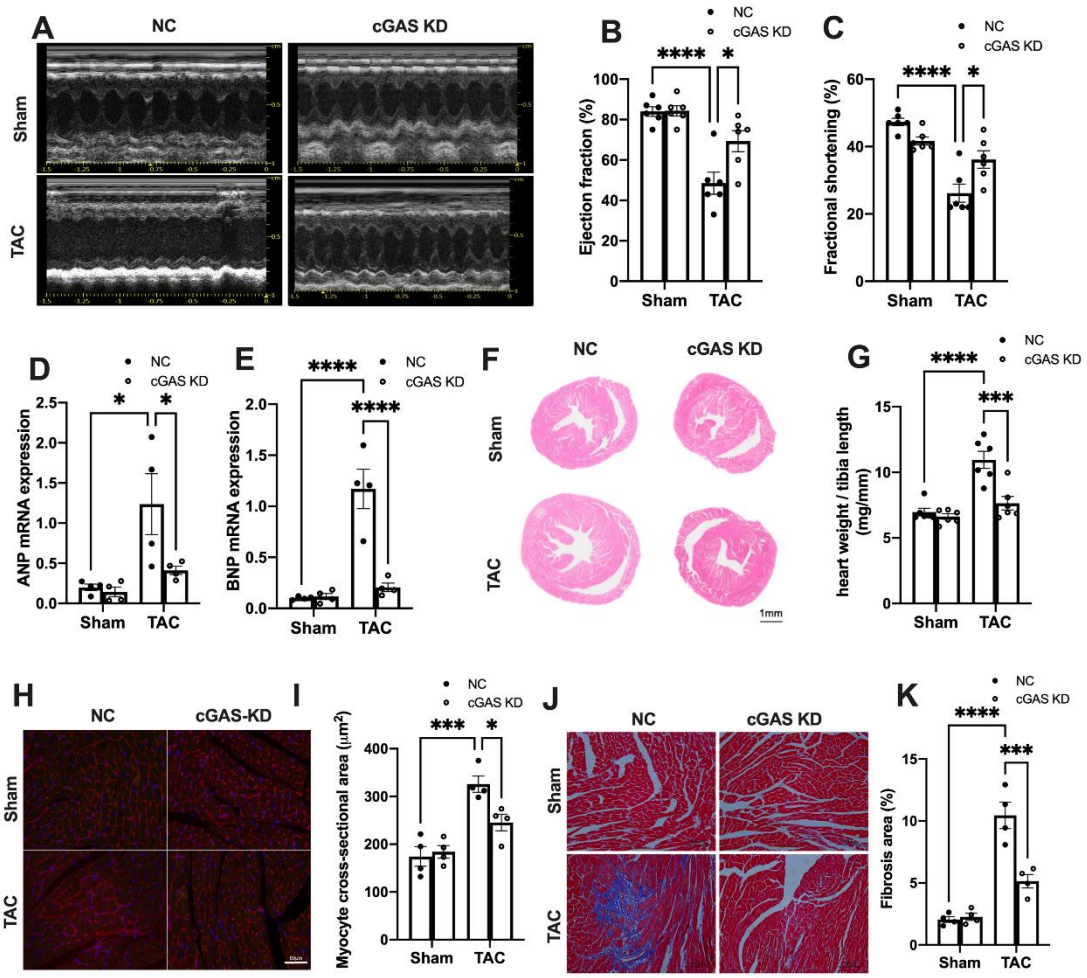

Figure S6. (A) cGAS knockdown improved cardiac function. Representative images of echocardiograms are presented. **(B-C)** LV ejection fraction and fractional shortening are shown in, n = 6. **(D-E)** cGAS knockdown reduced the mRNA expression levels of ANP and BNP in the heart from TAC mice, n = 4. **(F)** Representative hematoxylin-eosin staining of myocardial tissue. Scale bar: 1 mm. **(G)** HW/TL ratio as a measure of cardiac hypertrophy, n = 6. **(H)** Representative WGA staining to assess hypertrophy of cardiac myocytes. Scale bar: 100 μm. **(I)** Quantitative analysis of WGA staining, n = 6. **(J)** Representative images of Masson staining of the heart sections. Scale bar: 100 μm. the results of statistical analysis are shown in **(K)**, n = 4. Data are presented as the mean ± SEM. Data were analyzed using a two-way ANOVA with a Tukey's multiple-comparison post-hoc test. *, $P < 0.05$. **, $P < 0.01$. ***, $P < 0.001$. ****, $P < 0.0001$.

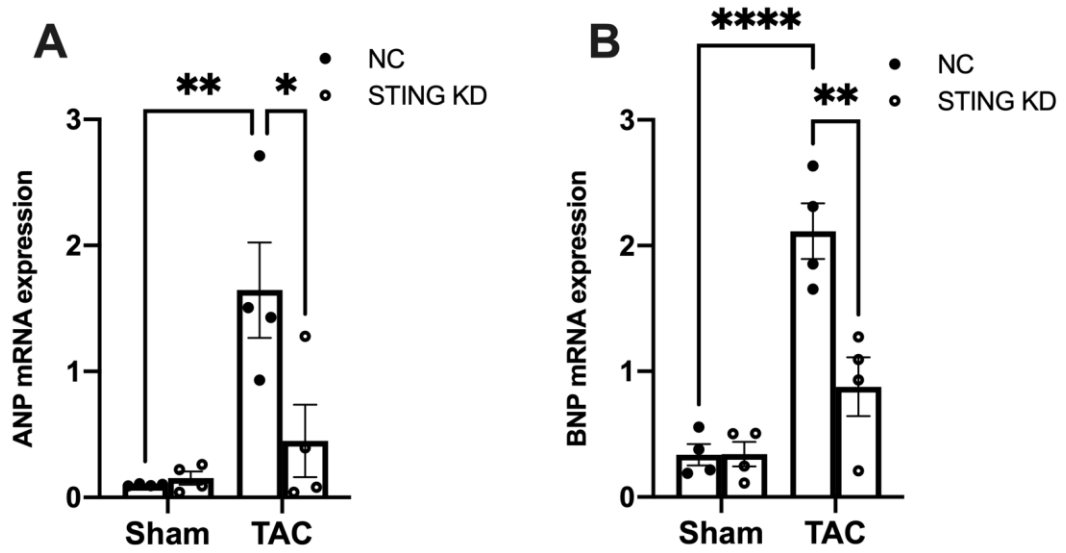

Figure S7. (A-B) cGAS knockdown reduced the mRNA expression of ANP and BNP in the heart from the TAC mice, n = 4. Data are presented as the mean ± SEM. Data were analyzed using a two-way ANOVA with a Tukey's multiple-comparison post-hoc test. *, $P < 0.05$. **, $P < 0.01$. ***, $P < 0.001$. ****, $P < 0.0001$.

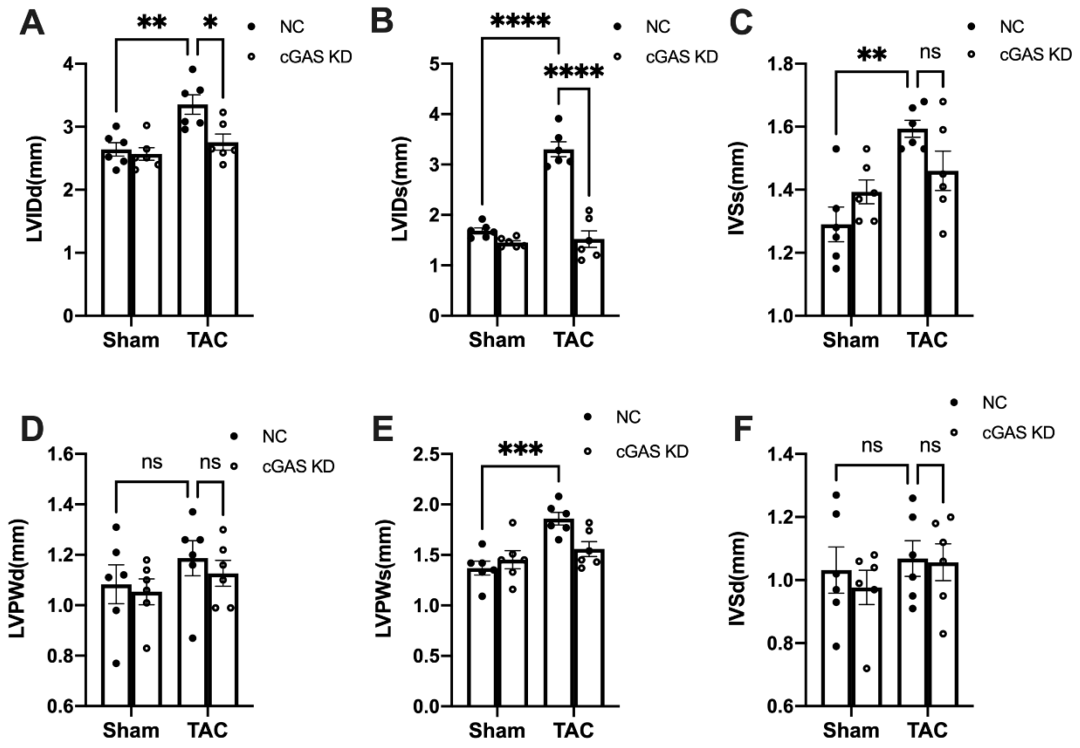

Figure S8. cGAS knockdown protected cardiac function against pressure overload. LVIDd **(A)**, LVIDs **(B)**, IVSs **(C)**, LVPWd **(D),** LVPWs **(E)** and IVSd **(F)** were measured with echo, n = 6. Data are presented as the mean ± SEM. Data were analyzed using a two-way ANOVA with a Tukey's multiple-comparison post-hoc test. LVIDd, end-diastolic left ventricular internal diameter; LVIDs, end-systolic left ventricular internal diameter; IVSd, end-diastolic interventricular septal thickness; IVSs, end-systolic interventricular septal thickness; LVPWd, end-diastolic left ventricular posterior wall thickness; LVPWs, end-systolic left ventricular posterior wall thickness. *, $P < 0.05$. **, $P < 0.01$. ***, $P < 0.001$. ****, $P < 0.0001$. ns indicates no significant.

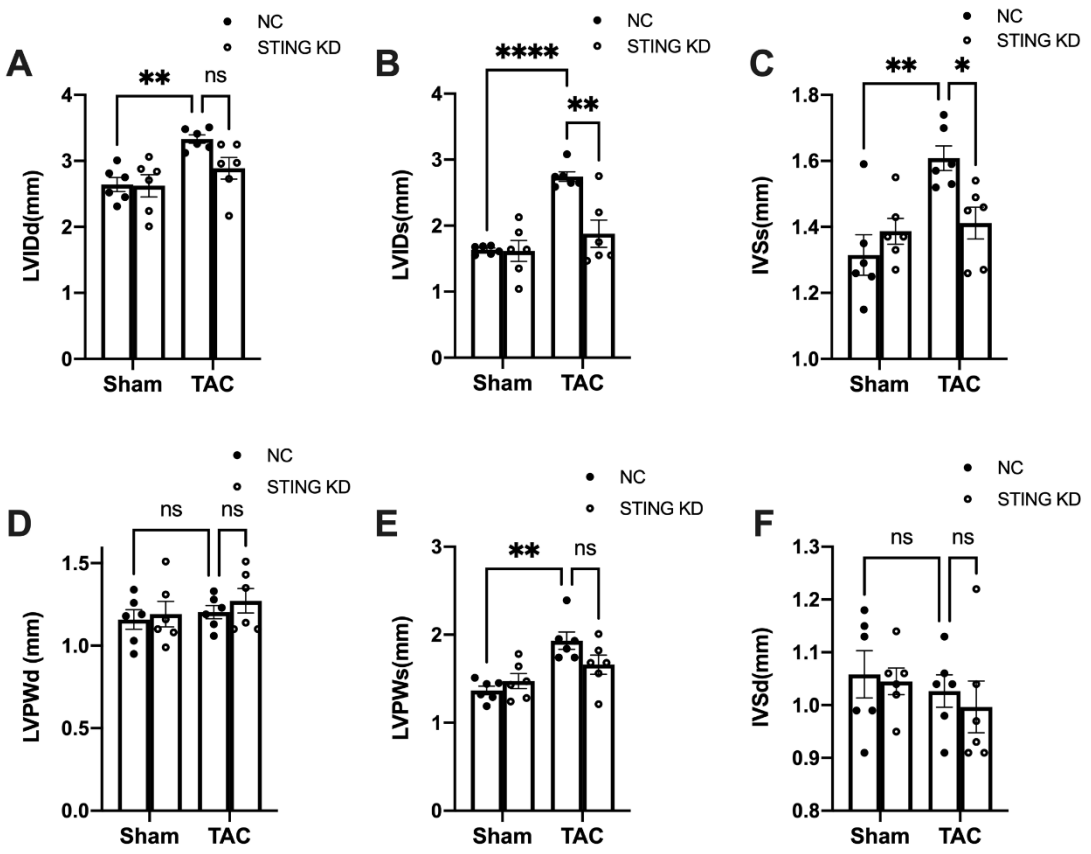

Figure S9. cGAS knockdown protects cardiac function against pressure overload. LVIDd **(A)**, LVIDs **(B)**, IVSs **(C)**, LVPWd **(D),** LVPWs **(E)** and IVSd **(F)** were measured with echo, n = 6. Data are presented as the mean ± SEM. Data were analyzed using a two-way ANOVA with a Tukey's multiple-comparison post-hoc test. LVIDd, end-diastolic left ventricular internal diameter; LVIDs, end-systolic left ventricular internal diameter; IVSd, end-diastolic interventricular septal thickness; IVSs, end-systolic interventricular septal thickness; LVPWd, end-diastolic left ventricular posterior wall thickness; LVPWs, end-systolic left ventricular posterior wall thickness. *, $P < 0.05$. **, $P < 0.01$. ****, $P < 0.0001$. ns indicates no significant.

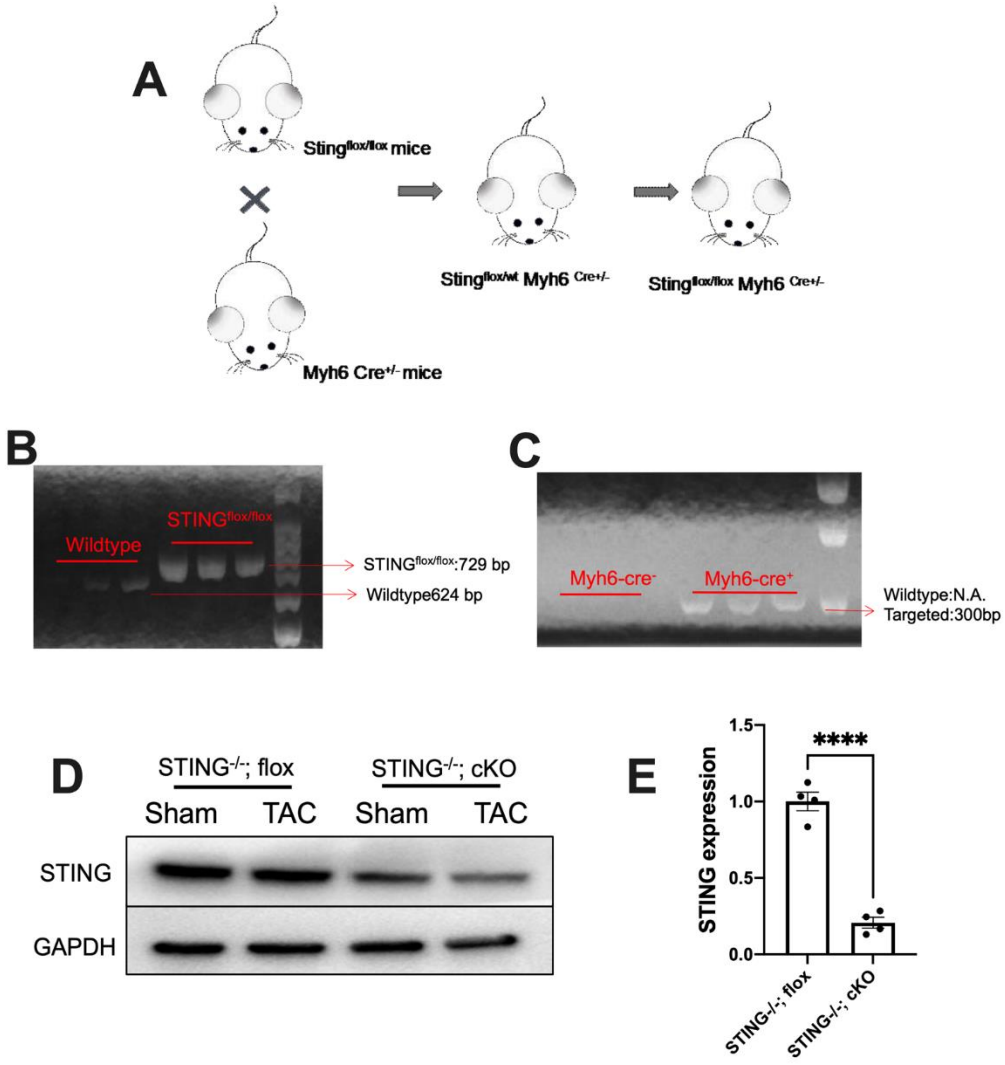

Figure S10. The generation of cardiomyocyte-specific STING deficient mice. **(A)** Schematic view of generation of cardiomyocyte-specific STING depletion mice (STING cKO mice). **(B-C)** Genotyping of STING cKO mice using PCR analysis. **(D-E)** The efficiency of STING depletion was measured with Western Blot, n = 4. Data are presented as the mean ± SEM. Data were analyzed using student *t* test. ****, $P < 0.0001$.

Supplemental Table S1: The used Real-time PCR primers in this study.

Primers	Forward	Reverse
Ccl2	CAGCCAGATGCAGTTAACGC	GCCTACTCATTGGGATCATCTTG
IFNβ1	CTGCGTTCCTGCTGTGCTTCTCCA	GAAGTCCGCCCTGTAGGTGAGGTTGA
IL6	TCCATCCAGTTGCCTTCTTG	GGTCTGTTGGGAGTGGTATC
Cxcl10	TTTCTGCCTCATCCTGCTGGGTCTGA	TGTGCGTGGCTTCACTCCAGTTAAGG
Irf7	GAGCGAAGAGGCTGGAAGACCAACTT	GCAGAACCTGTGTGGGCAGAGCATT
Ifit1	AGGCTGGAGTGTGCTGAGATGGACTG	TGTGCTGCTGAGGGCTTCTTCAATGT
Ifit2	CAGAGGAAGAGGTTGCCTGGAGAGTG	CTTGGTCAGGATGCTGTTGCTGGATG
Ifit3	CCTGGCACCATGAACCTGAGGACAAC	CCATAAGCAGCACTCCACAGCACATC
Osal2	TCAGCAGCAGGAAGACCCTAGCAGAT	GCACGGACTCAAGCAGCCAGACTA
GAPDH	ATGGTGAAGGTCGGTGTGAACGGATT	GTCTCGCTCCTGGAAGATGGTGATGG
ANP	GCTTCCAGGCCATATTGGAG	GGGGGCATGACCTCATCTT
BNP	GAGGTCACTCCTATCCTCTGG	GAGGTCACTCCTATCCTCTGG
Col1	GCTCCTCTTAGGGGCCACT	ATTGGGGACCCTTAGGCCAT
Col3	CTGTAACATGGAAACTGGGGAAA	CCATAGCTGAACTGAAAACCACC
Dloop1	AATCTACCATCCTCCGTGAAACC	TCAGTTTAGCTACCCCCAAGTTTAA
Dloop2	CCCTTCCCCATTTGGTCT	TGGTTTCACGGAGGATGG
Dloop3	TCCTCCGTGAAACCAACAA	AGCGAGAAGAGGGGCATT